Green synthesis of silver nanoparticles using *Terminalia cuneata* and its catalytic action in reduction of direct yellow-12 dye

Thomas Nesakumar Jebakumar Immanuel Edison, Yong Rok Lee, Mathur Gopalakrishnan Sethuraman

PII: S1386-1425(16)30101-9
DOI: doi: 10.1016/j.saa.2016.02.044
Reference: SAA 14310

To appear in:

Received date: 16 April 2015
Revised date: 2 July 2015
Accepted date: 28 February 2016

Please cite this article as: Thomas Nesakumar Jebakumar Immanuel Edison, Yong Rok Lee, Mathur Gopalakrishnan Sethuraman, Green synthesis of silver nanoparticles using *Terminalia cuneata* and its catalytic action in reduction of direct yellow-12 dye, (2016), doi: 10.1016/j.saa.2016.02.044

Green synthesis of silver nanoparticles using *Terminalia cuneata* and its catalytic action in reduction of direct yellow-12 dye

Thomas Nesakumar Jebakumar Immanuel Edison [a,b] Yong Rok Lee [a]* and Mathur Gopalakrishnan Sethuraman[b]**

[a] School of Chemical Engineering, Yeungnam University,

Gyeongsan – 712-749, Republic of Korea

[b] Department of Chemistry, Gandhigram Rural Institute – Deemed University,

Gandhigram – 624 302, Tamil Nadu, India

Abstract

Facile green synthesis of silver nanoparticles (AgNPs) using aqueous bark extract of *Terminalia cuneata* has reported in this article. The effects of concentration of the extract, reaction time and pH were studied by UV-Vis spectroscopy. Appearance of yellow color with λ_{max} around ~420 nm suggested the formation of AgNPs. The stable AgNPs were further characterized by Fourier transform infrared (FT-IR) spectroscopy, X-ray diffraction (XRD), Dynamic light scattering (DLS) with zeta potential and high resolution transmission electron microscopy (HR-TEM) with energy dispersive X-ray spectroscopy (EDS) analysis. The synthesized AgNPs were in size ranging of 25-50 nm with distorted spherical shape identified from HR-TEM analysis. The catalytic activity of AgNPs on the reduction of direct yellow-12 using $NaBH_4$ was analyzed using UV-Vis spectrophotometer. This study showed the efficacy of biogenic AgNPs in catalyzing the reduction of direct yellow-12.

Keywords

Silver nanoparticles; Green Synthesis; *Terminalia cuneata* bark; Catalyst; Direct yellow-12.

Authors for correspondence

**Prof. M.G. Sethuraman

E-mail: mgsethu@gmail.com

Tel: +914512452371; Mobile: +919443021565

*Prof. Y. R. Lee

E-mail: yrlee@yu.ac.kr

Fax: +82-53-810-4631; Tel: +82-53-810-2529

1.0 Introduction

Nanoscience has blossomed in the recent decades owing to its immense contribution in diverse fields like sensors, catalysts and medicine [1]. The electronic, optical and chemical properties of nanoparticles are entirely different from those of bulk of the same materials [2]. Among the nanoparticles, silver nanoparticles are of great interest of researchers due to its applications towards medical, catalysis, optics and energy fields. Generally colloidal metal nanoparticles are synthesized by chemical reduction of metal ions by reducing and capping agents. The principal advantages of the reduction method are facile fabrication of nanoparticles with various sizes and shapes viz., nanorods, nanowires, nanoprisms and nanoplates [3]. Polymers and surfactants are served as capping agents for protecting the metal nanoparticles from aggregation. Some of the reducing and capping agents are toxic to human beings and the environment. To overcome this problem, researchers have started to synthesis nanoparticles using bio sources such as microorganisms, fungi and plant extracts [4-9]. This method is very easy, environment benign and cost effective. Moreover, different sizes and shapes of nanoparticles can also be synthesized [10].

Direct yellow-12, an anionic azo dye, is readily soluble in polar solvents viz., water, methanol and ethanol, and utilized in different processes including silk, wool, leather, jute, cotton dyeing and paper printing. Direct yellow-12 dye must be present in the effluents of these industries [11]. Direct yellow-12 dye is quite toxic to humans and all aquatic organisms, the reduction of direct yellow-12 are industrially and environmentally important.

In the present work, AgNPs were synthesized using aqueous bark extract of *Terminalia cuneata*. It is otherwise known as *Arjun* tree (Fig. 1) belonging to *Combretaceae* family. The

major phytoconstituents present in the bark are tannins, triterpenoid saponins (arjunic acid, arjunolic acid and arjungenin), flavonoids, gallic acid, ellagic acid and phytosterols [12, 13].

The formation of AgNPs and effect of concentration, reaction time, pH of the reaction medium on AgNPs formation were analyzed by UV-Vis spectroscopy. The stable AgNPs were further characterized by FT-IR, XRD, DLS with zeta potential and HR-TEM with EDS analysis.

The stable AgNPs were utilized as a catalyst for the reduction of carcinogenic direct yellow-12 dye using $NaBH_4$ as reducing agent. The catalytic activity of AgNPs was analyzed by decrease in absorbance intensity of the dye at different time intervals using UV-Vis spectrophotometer.

Fig. 1

2.0 Materials and Methods

2.1 Preparation of *T. cuneata* bark extract

T. cuneata barks were collected from Gandhigram Rural Institute campus, dried and powdered. 0.50 g of the powdered bark was extracted with 100 ml of distilled water at 80˚ C for 15 min. The extract was filtered using Whatman No. 2 filter paper. Further, the filtrate was used as reducing source for the synthesis of AgNPs.

2.2 Synthesis of AgNPs using *T. cuneata*

The synthesis of AgNPs were carried out by taking different concentrations of *T. cuneata* extract viz., 0.50, 1.00, 1.75, 2.00 and 2.50 ml and adding to 24.50, 24.00, 23.25, 23.00 and 22.50 ml of 0.01 M $AgNO_3$ (CDH Chemicals, Mumbai, India) solutions respectively at room temperature. The total volume of the reaction was fixed as 25.00 ml.

2.3 Characterization of AgNPs

2.3.1 UV-Vis spectroscopy

The formation of AgNPs was studied using Perkin Elmer Lamda 35 UV-Vis spectrophotometer. The surface plasmon resonance (SPR) peak was observed in the range of 400-450 nm in visible region. The λ_{max} values were recorded after 10 min of reaction time as well as after 24 h so as to find out the stability of the biogenic AgNPs.

The effect of change of pH was studied by taking 1.75 mL of the bark extract of *T. cuneata* and adding to 23.25 mL of 0.01 M $AgNO_3$ at a given pH value. The pH was varied by the addition of 0.1 M sulphuric acid in the acidic region and 0.1 M sodium hydroxide solution in the basic region. The SPR peaks were recorded as before at various pH ranges such as 5, 6, 7, 8 and 9.

For UV-Vis spectroscopic studies, 0.30 ml of AgNPs was taken in a cuvette and diluted it to 2.00 ml by the addition of double distilled water. The absorbance of AgNPs was measured in the wavelength range between 200 – 800 nm.

2.3.2 FT-IR spectroscopy

The functional groups present in the phytoconstituents on the bark extract of *T. cuneata* and their involvement in the synthesis of AgNPs was determined by the FT-IR studies. The dried aqueous extract and synthesized AgNPs were mixed with KBr to make pellet and the FT-IR analysis was carried out by JASCO FT-IR 400.

2.3.3 XRD studies

The phytoreduced silver colloidal solution was drop-coated onto a glass substrate and the XRD measurements were carried out using a Philips X'Pert Pro X-Ray diffractometer, with the following working conditions: CuKα Ni-filtered radiation; 40 kV, 30 mA; divergence slit 0.47°.

2.3.4 Dynamic Light Scattering (DLS) and zeta potential measurements

In order to find out the stability and size distribution of AgNPs, the DLS and zeta potential measurements were carried out using Zetasizer Nano S90 (Malvern).

2.3.5 HR-TEM with EDS analysis

The stable biogenic AgNPs were washed and diluted by distilled water to attain the absorbance range of 0.50 a.u. Further, one drop of diluted AgNPs was placed on carbon coated Cu grid and allowed to dry *in-vacuo*. After drying, the nanoparticles were visualized using JEOL JEM 2100 high resolution transmission electron microscope at 200 kV of acceleration. Simultaneously the energy dispersive spectrum (EDS) was also recorded.

2.4 Evaluation of the effect of stable AgNPs on the reduction of direct yellow-12 by $NaBH_4$

Direct yellow-12 dye purchased from CDH Chemicals, India was used for this study. To find out the catalytic activity of synthesized AgNPs, two reactions were carried out in a 3.50 ml capacity quartz cuvette and absorbance values were monitored using UV-Vis spectrophotometer. In the first reaction, 1 ml of direct yellow-12 (0.5×10^{-3} M) was mixed with 0.2 ml stable AgNPs and 1.8 ml of freshly prepared $NaBH_4$ (0.1×10^{-2} M). Further the control reaction was also carried out without AgNPs. The reactions were continuously monitored by Perkin Elmer Lamda 35 UV-Vis spectrophotometer.

3.0 Results and Discussion

3.1 UV-Vis spectroscopy

AgNPs have optical properties and are sensitive to size, shape, concentration, agglomeration state and refractive index near the nanoparticle surface, which makes UV-Vis spectroscopy a valuable tool for identifying, characterizing and studying these AgNPs [14]. After addition of different concentrations of the bark extract of *T. cuneata* to Ag^+ solution, a visible color change

(appearance of yellow color) was noticed. This indicates the formation of AgNPs [15]. The intensity of the color increased while increasing the concentration of the extract and also the reaction time [16]. After 24 h, the color intensity was even higher, giving it a dark look. This clearly showed that the production of AgNPs increased with increase of concentration of extract and time. The UV-Vis spectrum recorded beyond 24 h did not show much increase in the absorbance.

UV-Vis spectra of synthesized AgNPs at different concentrations of the extract at two different time intervals (10 min and 24 h) are shown in Fig. 2 and Fig. 3

Fig. 2 and Fig. 3

From the Figures, it can be seen that the sharp SPR peak for AgNPs appeared around 415 nm (at 10 min), which suggested that the spherical shapes of AgNPs [17]. Further, the SPR was shifted to 422 nm on increasing of reaction time (24 h), suggesting that the size of AgNPs increased upon increasing the reaction time [18]. AgNPs produced from *T. cuneata* were observed to be very stable in solution, even after 3 months of synthesis.

The synthesis of nano-crystalline AgNPs using *T. cuneata* bark extract was tested over a wider pH ranges from 5–9. The UV-Vis spectrum of AgNPs synthesized at different pH values at two different time intervals are shown in Fig. 4 and 5. From the Fig. 4, SPR peak appeared at 417 nm in the acidic pH. While increasing the pH of the reaction, the SPR peak was shifted to lower wavelength which suggested that large nanoparticles are formed at lower pH, whereas highly dispersed, small nanoparticles are formed at high pH. At low pH, the aggregation of Ag nanoparticles to form larger nanoparticles was believed to be favored over the nucleation to form

new nanoparticles. At higher pH, a large number of AgNPs with smaller diameters are formed [19].

From the Fig. 5, it could be inferred that, the SPR peak of AgNPs appeared at 420 nm in the acidic region, which suggested the increasing of particle size with increasing of reaction time. In the basic region, a blue shift was observed. Moreover at pH-9 after 24 h of reaction time, two SPR peaks could be observed in the range of 399 nm and 545 nm. SPR peak at 545 nm could be attributed to the formation of anisotropic structures [20].

Fig. 4 and Fig. 5

It is a known fact that metal nanoparticles need to be stabilized through an appropriate capping agent. Plant extracts have been reported to function as reducing agents and stabilizing agents in the synthesis of nanoparticles [21]. Bulut and his coworker had elaborated on the capping mechanism of hydrolysable tannins which are the common phytoconstituents [22]. These tannins which are polyhydroxylated macromolecules, characterized by supra molecular associations facilitated by hydrogen bonding, act as templates for nanoparticle growth. The UV-Vis spectrum recorded after 24 h of reaction time clearly explains the stability of the biogenic AgNPs which can also be ascribed to the presence of polyphenols, tannins and gallic acid present as phytoconstituents in *T. cuneata*.

3.2 FT-IR spectroscopy

The FT-IR spectrum of dried aqueous *T. cuneata* extract and synthesized AgNPs are shown in Fig. 6. The main chemical constituents present in the bark are tannins, triterpenoid saponins (arjunic acid, arjunolic acid and arjungenin), flavonoids, gallic acid, ellagic acid and phytosterols [12]. The FT-IR-spectrum of *T. cuneata* bark extract showed an absorption band at

3385 cm^{-1} which is characteristic of the –OH stretching of hydrogen bonded phenolic group present in the phytoconstituents. The band at 1625 cm^{-1} was assigned to C=C stretching vibration of the phytoconstituents. The band at 1050 cm^{-1} was due to the vibrations of –C-O group of constituents and the band at 1440 cm^{-1} could be due to aromatic –CH stretching vibrations. Further, the IR spectra of biogenic AgNPs showed an absorption band at 1383 cm^{-1}, corresponding to $–NO_3$ stretching comes from silver nitrate [23]. Comparison of the FT-IR spectra of biogenic AgNPs with that of the aqueous extract revealed that these major phytoconstituents are indeed responsible for the capping of AgNPs.

Fig. 6

3.3 XRD studies

As a primary characterization tool for obtaining critical features such as crystal structure, crystallite size and strain, X-ray diffraction patterns have been widely used in nanoparticle research. The XRD pattern of synthesized AgNPs using *T. cuneata* is shown in Fig. 7. There are four major peaks appeared at 38.2°, 44.5°, 64.5° and 77.6°. These peaks correspond to the (111), (200), (220) and (311) planes of face-centered-cubic (fcc) geometry of AgNPs, which is in agreement with the JCPDS file No. 42-0783. The ratio between the intensities of (111) and (200) diffraction peaks was relatively higher than the usual values which indicate that the experimental system had AgNPs oriented in (111) plane [24]. XRD pattern thus revealed the fcc geometry of AgNPs synthesized with mostly oriented in (111) plane.

Fig. 7

3.4 DLS with zeta potential analysis

The particle size distribution of AgNPs in solution was directly determined by DLS measurements. The size distribution images of stable AgNPs synthesized using *T. cuneata* is shown in Fig. 8. From the results, the calculated particle size distribution of AgNPs is 25-50 nm.

The zeta potential of stable AgNPs is calculated as -32.6 mV (pH-6.95) (Fig. 9). This suggests the high stability of biogenic AgNPs [25]. The large negative potential value could be due to the capping of polyphenolic constituents present in the plant extracts. In the colloidal solution, nitrate and gallate ions (from phytoconstituents) are present adsorbed on the surface of AgNPs. Hence as a result the surface charge of the Ag nanoparticles will be negative [26].

Fig. 8 and Fig. 9

3.5 HR-TEM with EDS analysis

The HR-TEM and SAED pattern of stable AgNPs synthesized using *T. cuneata* are depicted in Fig. 10. The calculated average particle size is approximately 25 nm. Further the synthesized AgNPs are mostly in distorted spherical shape. White dots in the SAED pattern of AgNPs revealed the crystalline nature. The EDS of stable AgNPs is shown in Fig. 11. From the figure, a strong signal of the Ag atoms is observed and the weak signals of O and C are also seen. Thus the TEM studies revealed the crystalline nature of the biogenic AgNPs and also the size of AgNPs.

Fig. 10 and Fig. 11

3.6 Mechanism of formation and protection of AgNPs by the phytoconstituents of *T. cuneata*

Proposing the mechanism of reduction of Ag^+ using phytoconstituents is very difficult, because they contain diverse molecular structures. Generally, in the synthesis of metal nanoparticles using plant extracts, the plant extracts play a dual role viz., reduction of metal ions and capping of metal nanoparticles (protection from aggregation) [27]. The plausible mechanism is represented in Fig. 12. In this mechanism, the optimum concentration of the extract for reduction and stabilization of AgNPs is taken in to account.

The phytoconstituents such as polyphenols, tannins and gallic acid contain high density of hydroxyl groups. On addition of extracts to the Ag^+ solution, the Ag^+-phytoconstituent complex was formed as intermediate. Further, the Ag^+ ions were converted to Ag atoms followed by coalescence, cluster formation and growth of clusters finally yielding AgNPs [22, 28]. The phenolic groups present in the phytoextract subsequently undergo oxidation and converted to its quinone form. The electrochemical potential difference between Ag^+ and phytoconstituents drives the reaction. The formed AgNPs were stabilized through the lone pair of electrons and pi electrons of quinone structures.

Fig. 12

3.7 Catalytic activity of AgNPs on reduction of direct yellow-12 by $NaBH_4$

The reduction of direct yellow-12 by $NaBH_4$ was also carried out using stable 25 nm sized biogenic AgNPs as a catalyst. Generally azo dyes are commonly prepared by coupling of a diazotized aromatic amine with a phenol or aromatic amine. It is often subjected to reductive or oxidative processes to remove color. Recently, an investigation of the ability of aqueous $Na_2S_2O_4$

and $SnCl_2$ for reductive cleavage of azo dyes resulted in nearly complete reduction of the azo bond to form the corresponding amines [29]. Generally, direct yellow-12 shows absorption maxima in the range of 404 nm. After addition of stable AgNPs to the reaction mixture containing direct yellow-12 and $NaBH_4$, color of the dye gradually disappeared. Complete decolorization of direct yellow-12 could be observed within 40 min after the reaction commenced (Fig. 13). It was inferred that in the absence of AgNPs and $NaBH_4$, the decolorization (reduction) of direct yellow-12 did not occur. This reaction is not kinetically favored but it is thermodynamically favored in presence of metal catalysts [30-31].

The reduction of direct yellow-12 can be explained in terms of Langmuir–Hinshelwood model [32-33]. In this reduction, $NaBH_4$ act as electron donor as well as hydrogen supplier in addition that, it also changed the pH of the entire solution [34]. Hence the surface charge of AgNPs changed to positive. The BH_4^- and direct yellow-12 are concomitantly adsorbed on the positively charged AgNPs surface. Then the catalytic reduction is started by relaying electrons from the donor BH_4^- to direct yellow-12, where the AgNPs accept electrons from BH_4^- ions and convey them to the dye molecule [35]. In the presence of AgNPs, large volume of hydrogen supplied by $NaBH_4$ could result in the hydrogenation of azo dyes.

There are several reports available on the catalytic activity of noble metal particles in the reduction of azo dyes. Mohapatra *et al* had investigated the azo bond cleavage of methyl red via hydrogenation using Pt nanowires [36]. Pd nanoparticles generated using microbes were reported to degrade azo dyes via reductive hydrogenation of the azo linkage. Methyl orange was degraded to give N,N-Dimethyl-benzene-1,4-diamine and Sulfanilic acid as the products. Concomitantly generated hydrogen was proposed to be the cause for hydrogenation [37]. In the light of the above reports, it is suggested that in the degradation of direct yellow-12 by $NaBH_4$ in the

presence of biogenic AgNPs, the simultaneous cleavages of two azo bonds occur resulting in the formation of corresponding amines viz., 4-ethoxyaniline and disodium (E)-6,6'-(ethene-1,2-diyl)bis(3-aminobenzenesulfonate) (Fig. 14). This may due to large surface area of AgNPs which could offer more catalytic sites toward the reduction of direct yellow-12 as well as high negative potential of AgNPs (-1.80 V Vs NHE) [38].

Fig. 14

4.0 Conclusions

The study has demonstrated that AgNPs could be prepared instantly by making use of aqueous bark extract of *T. cuneata*. The phytoconstituents (mostly tannins and poly phenols) present in the extracts of *T. cuneata* act as reducing agents as well as capping agents providing stability to AgNPs as evident from FT-IR study. The phytosynthesized AgNPs were found to have a crystalline structure with face centered cubic geometry oriented in (111) plane as studied by XRD method. The synthesized AgNPs have the size ranging approximately 25-50 nm with distorted spherical shape as studied by HR-TEM and DLS studies. The high negative zeta potential values of AgNPs, confirmed the high stability. The biogenic AgNPs prepared using *T. cuneata* were tested for its efficacy in degrading direct yellow-12. The results of the study demonstrated the ability of biogenic AgNPs as excellent catalyst in the degradation of direct yellow-12.

References

[1] M.C. Roco, W.S. Bainbridge, J. Nanopart. Res. 7 (2005) 1.

[2] M. Brust, D.J. Schiffrin, D. Bethell, C.J. Kiely, Adv. Mater. 7 (1995) 795.

[3] J.E. Millstone, S. Park, K.L. Shuford, L. Qin, G.C. Schatz, C.A. Mirkin, J. Am. Chem. Soc. 127 (2005) 5312.

[4] Z. Sadowski, I.H. Maliszewska, B. Grochowalska, I. Polowczyk, T. Kozlecki, Mater. Sci-Poland 26 (2008) 419.

[5] E.E. Emeka, O.C. Ojiefoh, C. Aleruchi, L.A. Hassan, O.M. Christiana, M. Rebecca, E.O. Dare, A.E. Temitope, Micron 57 (2014) 1.

[6] S.M. Roopan, Rohit, G. Madhumitha, A.A. Rahuman, C. Kamaraj, A. Bharathi, T.V. Surendra, Ind. Crop. Prod. 43 (2013) 631.

[7] M. Vijayakumar, K. Priya, F.T. Nancy, A. Noorlidah, A.B.A. Ahmed, Ind. Crop. Prod. 41 (2013) 235.

[8] K. Krishnaswamy, H. Vali, V. Orsat, J. Food Eng. 142 (2014) 210.

[9] T. Wang, J. Lin, Z. Chen, M. Megharaj, R. Naidu, J. Clean. Prod. 83 (2014) 413.

[10] V.K. Sharma, R.A. Yngard, Y. Lin, Adv. Colloid Interface Sci. 145 (2009) 83.

[11] A. Rathi, H.K. Rajor, R.K. Sharma, J. Hazard Mater. 102 (2003) 231.

[12] V. Dhingra, S. Dhingra, A. Singla, Egypt. J. Forensic Sci. 3 (2013) 15.

[13] S. Dwivedi, J. Ethnopharmacol. 114 (2007) 114.

[14] K.G. Stamplecoskie, J.C. Scaiano, J. Am. Chem. Soc. 132 (2010) 1825.

[15] T.J.I. Edison, M.G. Sethuraman, Spectrochim. Acta A 104 (2013) 262.

[16] M. Sathishkumar, K. Sneha, S.W. Won, C.-W. Cho, S. Kim, Y.-S. Yun, Colloids Surf. B 73 (2009) 332.

[17] N.A. Negm, S.M. Tawfik, A. Abd-Elaal, J. Ind. Eng. Chem. (2015) 1051.

[18] A. Hebeish, M.H. El-Rafie, M.A. El-Sheikh, M.E. El-Naggar, J. Nanotechnol. (2013) Article ID 201057.

[19] S. Iravani, B. Zolfaghari, BioMed. Res. Int. (2013) Article ID 639725.

[20] B. Wiley, Y. Sun, B. Mayers, Y. Xia, Chem. Eur. J. 11 (2005) 454.

[21] V. Kumar, S.K. Yadav, J. Chem. Technol. Biotechnol. 84 (2009) 151.

[22] E. Bulut, M. Ozacar, Ind. Eng. Chem. Res. 48 (2009) 5686.

[23] J. Coates, Encyclopedia of analytical chemistry, R.A. Meyers (Ed.), John Wiley & Sons Ltd, Chichester, (2000) 10815–10837.

[24] Y. Zhu, X. Wanga, W. Guo, J. Wang, C. Wang, Ultrason. Sonochem. 17 (2010) 675.

[25] A. Gade, S. Gaikwad, N. Duran, M. Rai, Micron, 59 (2014) 52.

[26] I. Sondi, B. Salopek-Sondi, J. Colloid Interface Sci. 275 (2004) 177.

[27] S.S. Ravi, L.R. Christena, N. SaiSubramanian, S.P. Anthony, Analyst 138 (201) 4370-4377.

[28] T.J.I. Edison, M.G. Sethuraman, Process Biochem. 47 (2012) 1351.

[29] R.D. Voyksner, R. Straub, J.T. Keever, H.S. Freeman, W. Hsu, Environ. Sci. Technol. 27 (1993) 1665.

[30] Y. Zheng, A. Wang, J. Mater. Chem. 22 (2012) 16552.

[31] A. Gangula, R. Podila, M. Ramakrishna, L. Karanam, C. Janardhana, A.M. Rao, Langmuir 27 (2011) 15268.

[32] T. J. I. Edison, M. G. Sethuraman, Y. R. Lee, Res Chem Intermed DOI 10.1007/s11164-015-2051-0.

[33] S. Wunder, F. Polzer, Y. Lu, Y. Mei, M. Ballauff, J. Phys. Chem. C 114 (2010) 8814.

[34] Z. Dong, X. Le, Y. Liu, C. Dong, J. Ma, J. Mater. Chem. A, 2 (2014) 18775.

[35] V.K. Vidhu, D. Philip, Micron 56 (2014) 54.

[36] S.K. Mohapatra, S.U. Sonavane, R.V. Jayaram, P. Selvam, Org. Lett. 4 (2002) 4297.

[37] A. Johnson, G. Merilis, J. Hastings, M.E. Palmer, J.P. Fitts, D. Chidambaram, J. Electrochem. Soc. 160 (2013) G27.

[38] N. Pradhan, A. Pal, T. Pal, Colloids Surf. A. 196 (2002) 247.

Figure captions

Fig. 1 Photograph of *Terminalia cuneata* plant Inset: Barks of *T. cuneata*

Fig. 2 Effect of concentration of the *T. cuneata* extract on AgNPs synthesis (after 10 min)

Fig. 3 Effect of concentration of the *T. cuneata* extract on AgNPs synthesis (after 24 h)

Fig. 4 UV–Vis spectra of AgNPs prepared using *T. cuneata* at various pH ranges (after 10 min)

Fig. 5 UV–Vis spectra of AgNPs prepared using *T. cuneata* at various pH ranges (after 24 h)

Fig. 6 FT-IR spectra of aqueous fruit extract of *T. cuneata* (A) and synthesized AgNPs with capping of phytoconstituents of *T. cuneata* (B)

Fig. 7 XRD pattern of synthesized AgNPs using *T. cuneata* extract

Fig. 8 DLS size distribution of AgNPs synthesized using *T. cuneata* extract

Fig. 9 Zeta potential of AgNPs synthesized using *T. cuneata* extract

Fig. 10 HR-TEM and SAED images of AgNPs synthesized using *T. cuneata* under different magnifications

Fig. 11 EDS pattern of AgNPs synthesized using *T. cuneata* extract

Fig. 12 Mechanism of formation and protection of AgNPs by *T. cuneata*

Fig. 13 Reduction of direct yellow-12 by $NaBH_4$ in presence of AgNPs as a catalyst

Fig. 14 Catalytic action of AgNPs synthesized using *T. cuneata* on the reduction of direct yellow-12.

Figures

Fig. 1

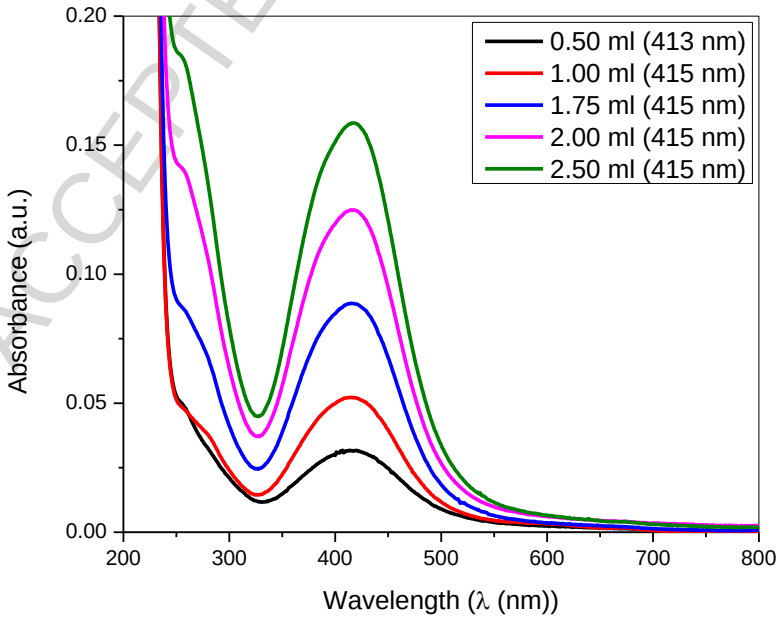

Fig. 2

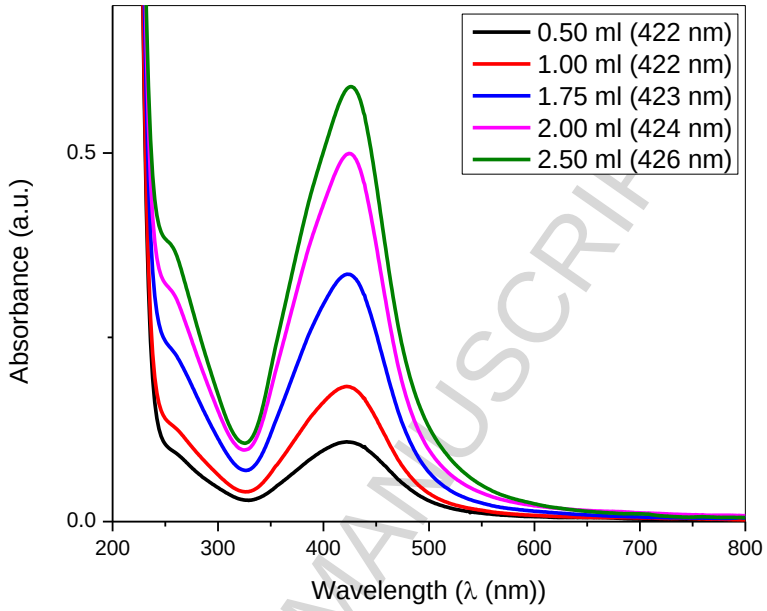

Fig. 3

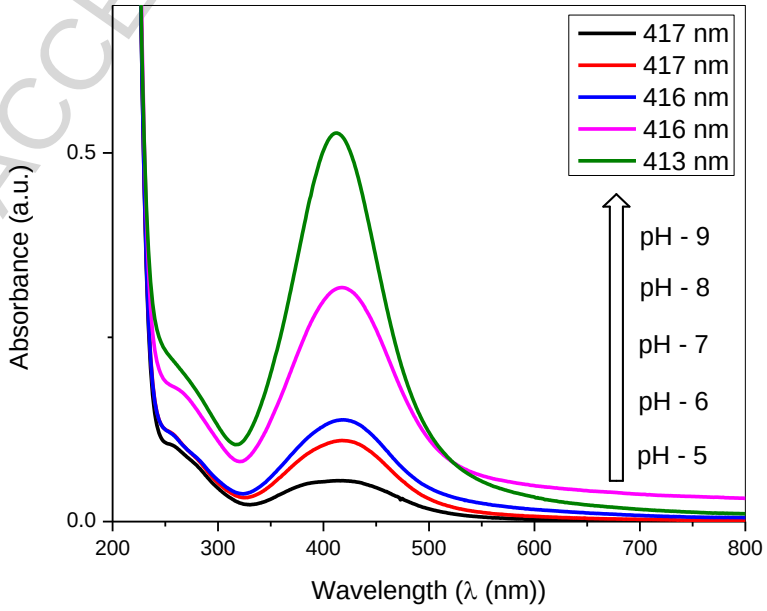

Fig. 4

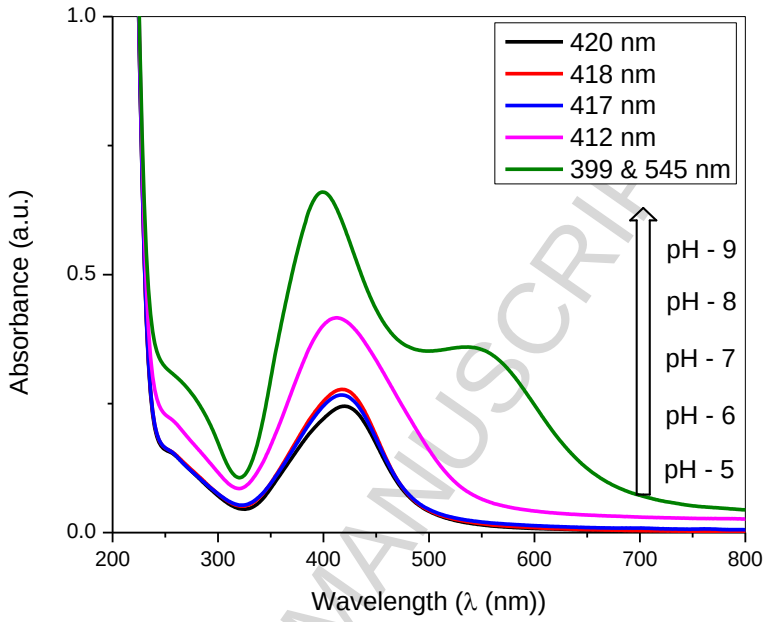

Fig. 5

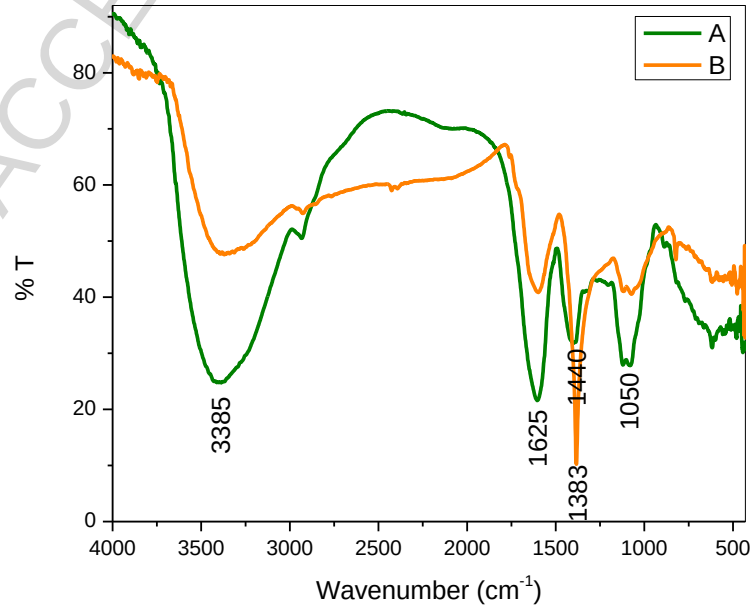

Fig. 6

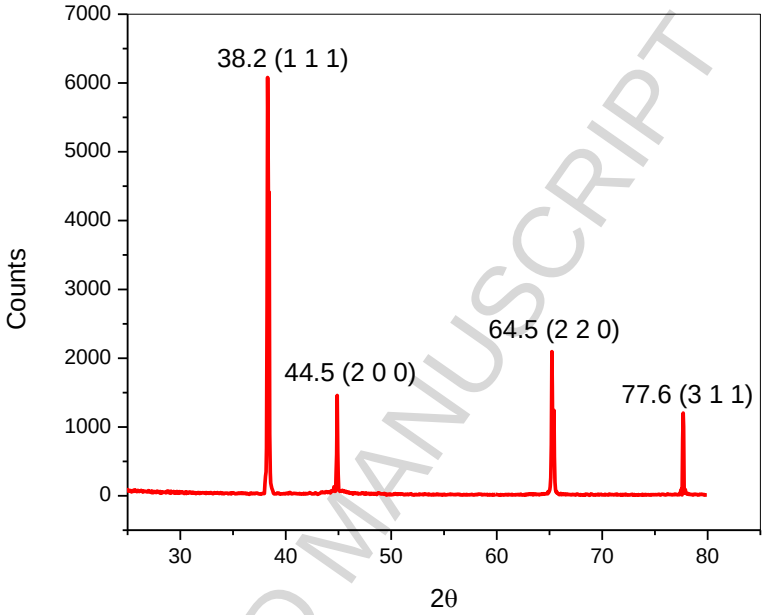

Fig. 7

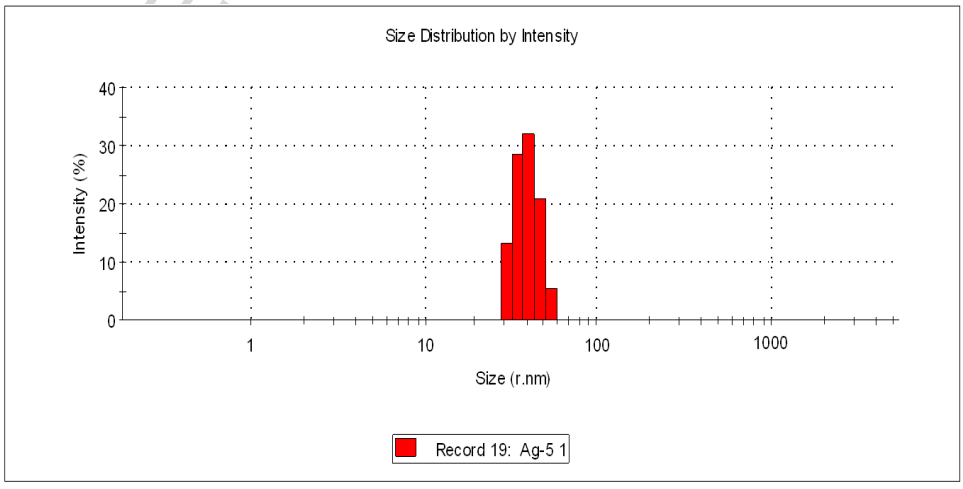

Fig. 8

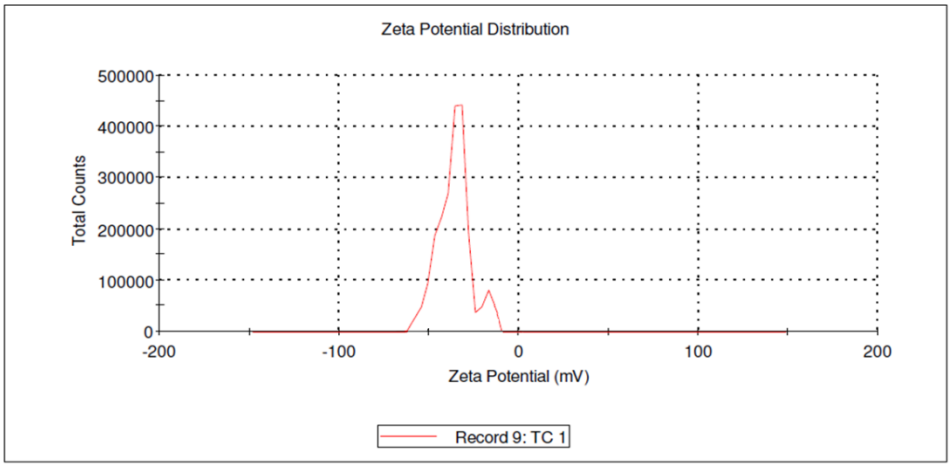

Fig. 9

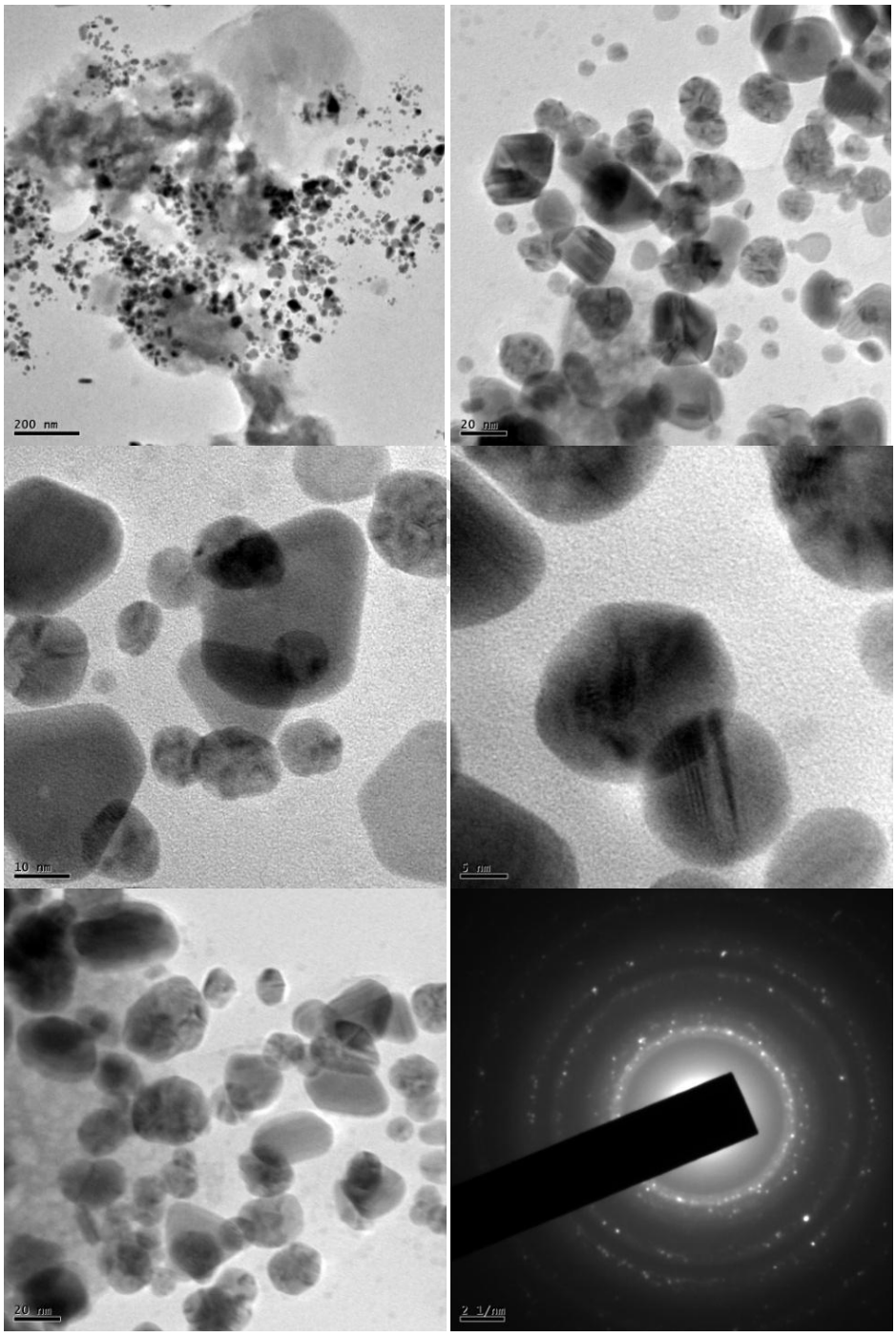

Fig. 10

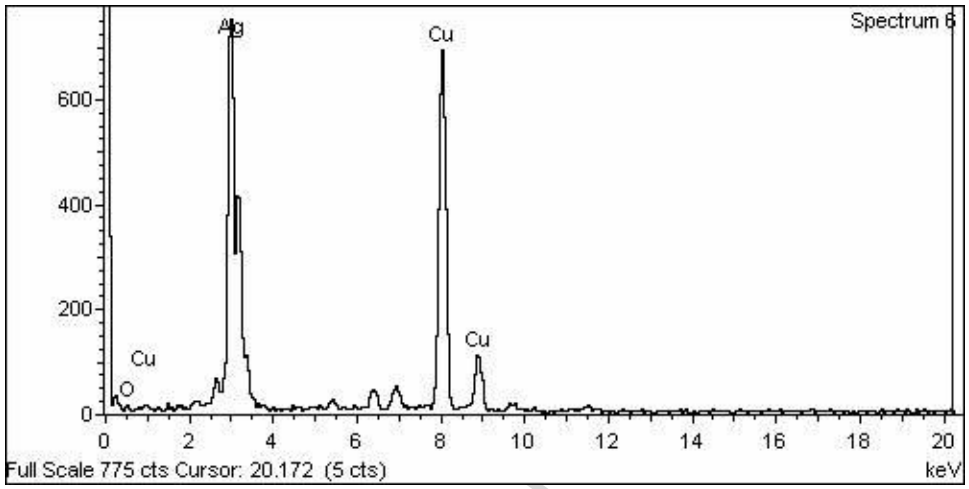

Fig. 11

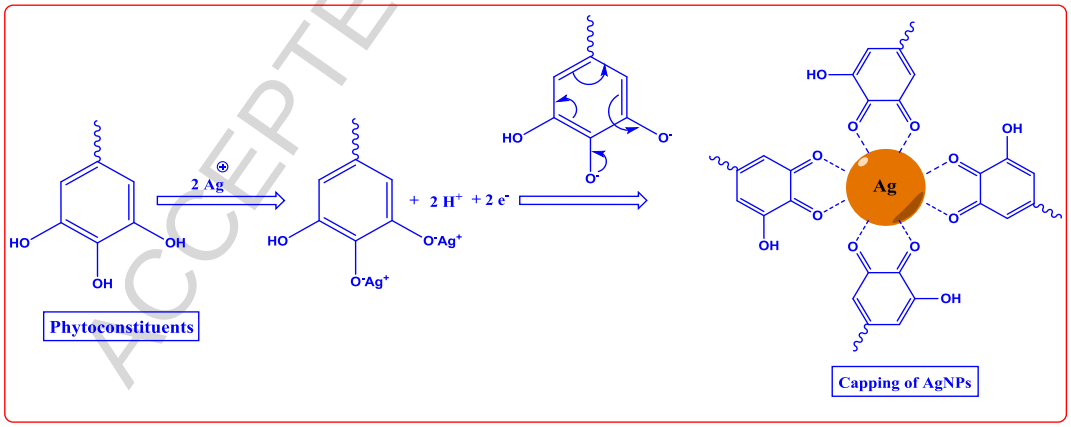

Fig. 12

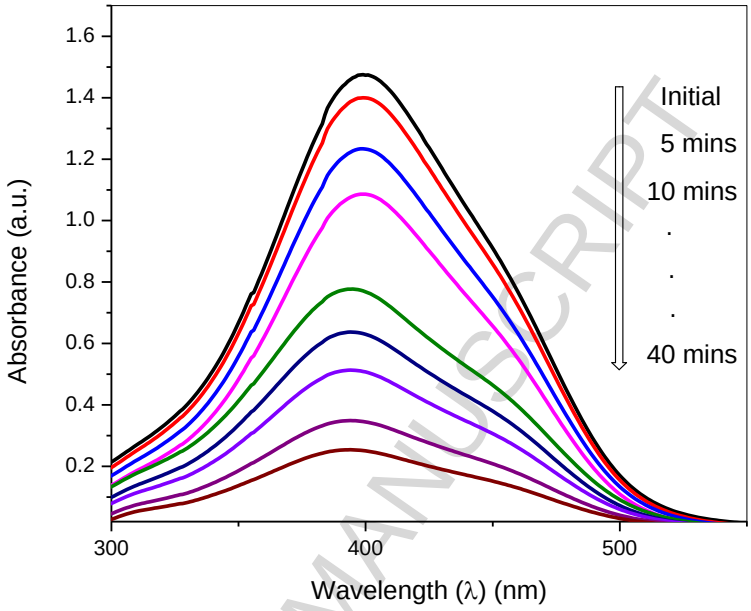

Fig. 13

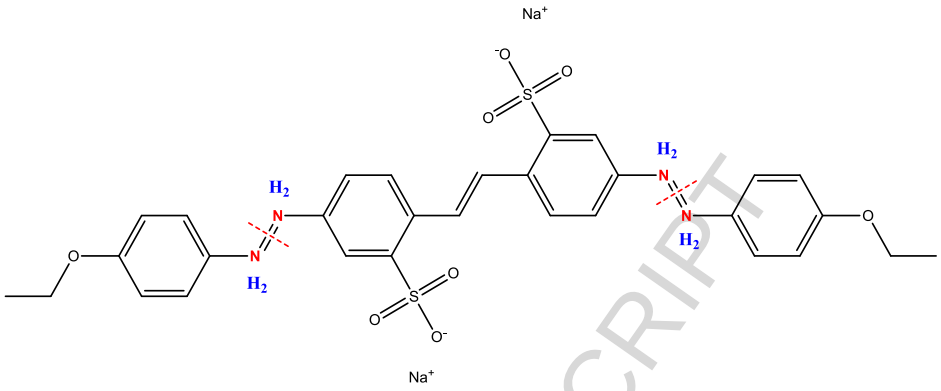

Disodium 4,4'-bis[(4-ethoxyphenyl)azo]stilbene-2,2'-disulphonate
(Direct Yellow 12)

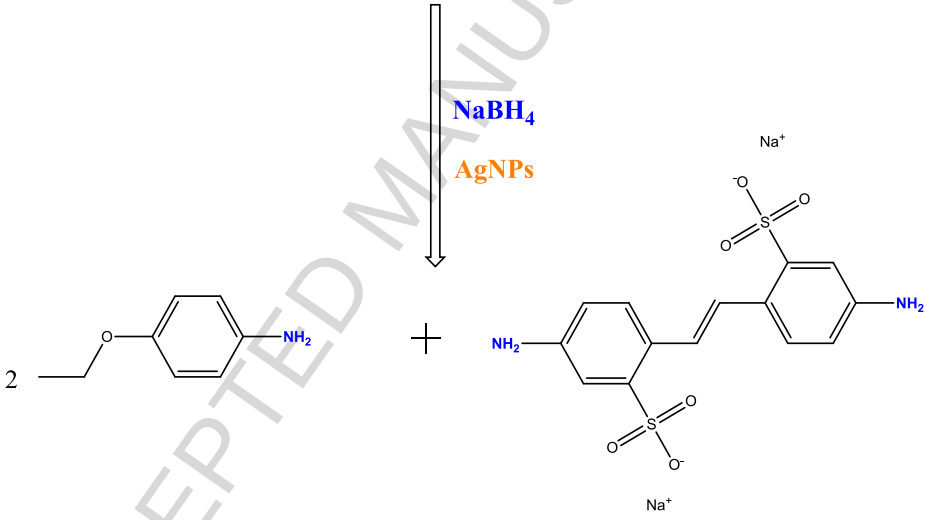

4-ethoxyaniline

Disodium (*E*)-6,6'-(ethene-1,2-diyl)bis(3-aminobenzenesulfonate)

Fig. 14

Green synthesis of silver nanoparticles using *Terminalia cuneata* and its catalytic action in reduction of direct yellow-12 dye

Thomas Nesakumar Jebakumar Immanuel Edison [a,b] Yong Rok Lee [a]* Mathur Gopalakrishnan Sethuraman [b]**

[a] School of Chemical Engineering, Yeungnam University,
Gyeongsan – 712-749, Republic of Korea

[b] Department of Chemistry, Gandhigram Rural Institute – Deemed University,
Gandhigram – 624 302, Tamil Nadu, India

Graphical Abstract

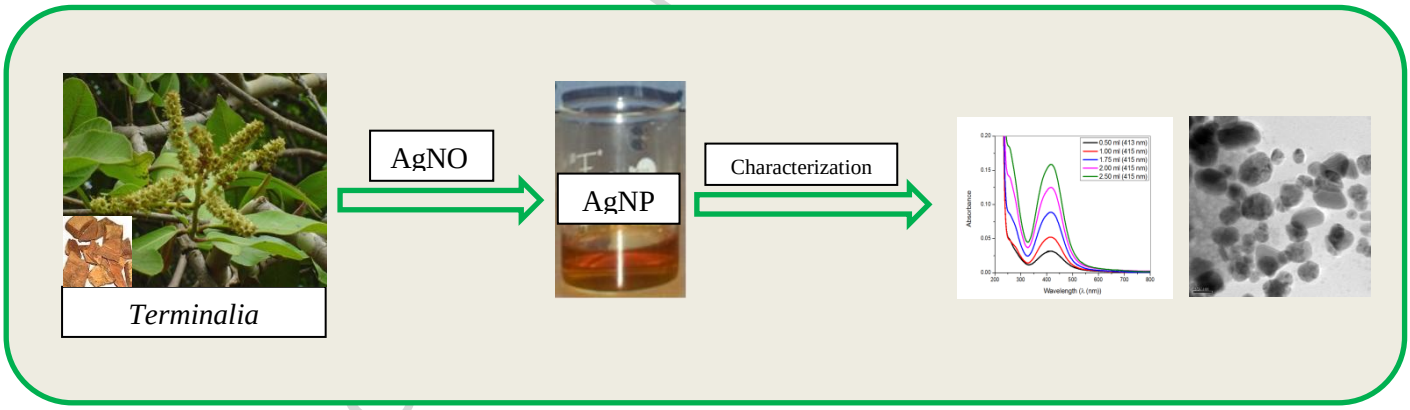

Highlights:

- Synthesis of silver nanoparticles using *Terminalia cuneata* bark is reported
- The size of the silver nanoparticles is in the range of 20-50 nm
- The catalytic reduction of direct yellow-12 was achieved using $NaBH_4$